Book of Tutorials and Abstracts

European
Microbeam Analysis Society

EMAS 2018

13th EMAS Regional Workshop

MICROBEAM ANALYSIS IN THE EARTH SCIENCES

4 - 7 September 2018
University of Bristol, Wills Hall, Bristol, Great Britain

Organised in collaboration with:
Mineralogical Society of Great Britain and Ireland
and
University of Bristol

ATOM PROBE TOMOGRAPHY: PROVIDING NEW INSIGHTS INTO GEOLOGICAL MATERIALS

J.O. Douglas, P.A.J. Bagot and M.P. Moody

University of Oxford, Department of Materials, Atom Probe Research Group
Parks Road, Oxford OX1 3PH, Great Britain
e-mail: james.douglas@materials.ox.ac.uk

ABSTRACT

Atom probe tomography (APT) is a material characterisation technique that combines sub-nm spatial resolution with high compositional sensitivity within typical analysis volumes of 80 nm x 80 nm x 200 nm. During APT, ions are evaporated from a needle shaped specimen through a voltage or laser pulse combined with a high standing voltage onto a 2D detector, giving both spatial and time-of-flight- information for each ion. This data is then reconstructed into a 3D point cloud of the original volume, providing a powerful visual tool for nanoscale analysis. Initially restricted to electrically conductive materials such as metals, the introduction of high speed laser pulsing has allowed the reliable analysis of semiconductors and insulators. Site specific focussed ion beam sample preparation, when combined with other electron microscopy techniques such as electron backscatter diffraction, transmission Kikuchi diffraction and energy-dispersive X-ray spectrometry, enable APT analysis of selected regions of materials with sub-micrometre precision.

Within this work, a general overview of APT will be presented as it applies to geological materials, discussing aspects of the sample preparation, analysis parameters and data reconstruction.

1. INTRODUCTION

Atom probe tomography (APT) is a time-of-flight mass spectrometry technique that uses the process of field evaporation to ionise surface atoms from a nanoscale needle shaped specimen and accelerate them towards a 2D position sensitive detector. The background of the technique and its application within modern instruments can be found in the literature [1, 2] but the fundamentals will be discussed here in brief.

A high standing field is applied to the sample to maintain the surface atoms almost at the point of evaporation, a further voltage or laser pulse is then applied in order to complete the evaporation process, allowing time of flight information to be collected. Typical fields experienced by these samples are in the 10s of V/nm range through the application of a few kV to the sample and pulse rates used are in the 100s of kHz.

Sample are kept at cryogenic temperatures (~50 K) in order to reduce surface atom mobility and are analysed in a high vacuum of ~10^{-11} Torr to reduced adsorbed contaminants on the surface of the sample, prevent gas atoms ionising in the high electric field and maintain a high mean free path. The sample itself is the main optic in this technique and there is an effective magnification of the order of a million times from the sample tip to the detector, giving spatial resolution up to 0.2 nm in the analysis direction and up to 0.5 nm in the plane of analysis. Detected ions are then back projected to form a 3D reconstruction of the detected ions.

APT operates within a region of spatial resolution and compositional sensitvity fills a characterisation niche between transmission electron microscopy (TEM) and secondary ion mass spectrometry (SIMS) techniques (as shown in Fig. 1), giving detection limts in the tens of ppm combined with sub-nm spatial resolution in typical volumes of 80 nm x 80 nm x 200 nm and consisting of tens of millions of ions.

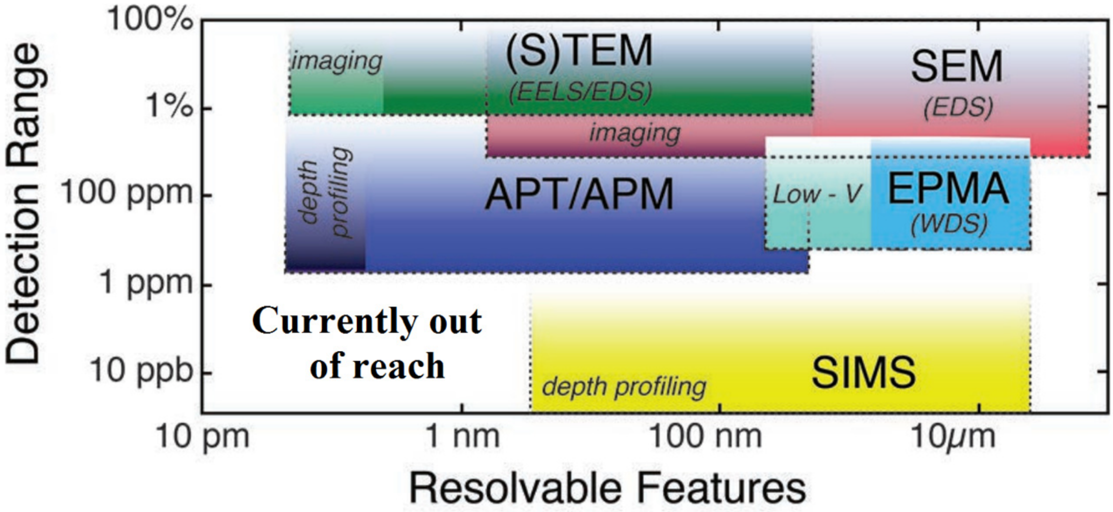

Figure 1. Spatial resolution and compositional detection limits for various microbeam techniques. Modified from [3].

2. *APT SAMPLE PREPARATION AND ANALYSIS*

There are two main methods of sample preparation for APT, electrochemical polishing and focussed ion beam (FIB) liftout. Electrochemical polishing is limited to those materials that can be readily etched into the required geometry, however this is not site specific and is often unsuitable for non-metals. This, combined with conductivity requirements for voltage pulsing, meant that initially atom probe analysis was restricted to conductive metals. Advances in laser pulsing [4], which added a thermal component to the field evaporation process [5], allowed the analysis of semiconducting [6] and insulating materials [7]. Laser wavelength, frequency and pulse energy can have significant impact on both the mass spectra detected, especially with species that have large differences in required evaporation field. Coating completed APT tips with nanoscale layers of conductive metal have been shown to improve electrical conductivity and yield [8], allowing insulating materials to be analysed with greater success.

Improvements in FIB technology, especially in modern dual beam focussed ion beam/scanning electron microscopes (FIB/SEM), has greatly increased the number of materials that can be prepared for APT. FIB sample preparation for APT has been adapted from TEM sample preparation and follows a general protocol of: deposition of a protective layer of material through electron beam/ion beam decomposed organometallic gas, trenching to form a wedge, lifting out the wedge using a micromanipulator and then milling to the required geometry [10]. Techniques such as electron backscatter diffraction (EBSD) [11] or energy-dispersive X-ray spectrometry (EDS) can be to location specific regions for liftout. A typical process flow can be seen in Fig. 2.

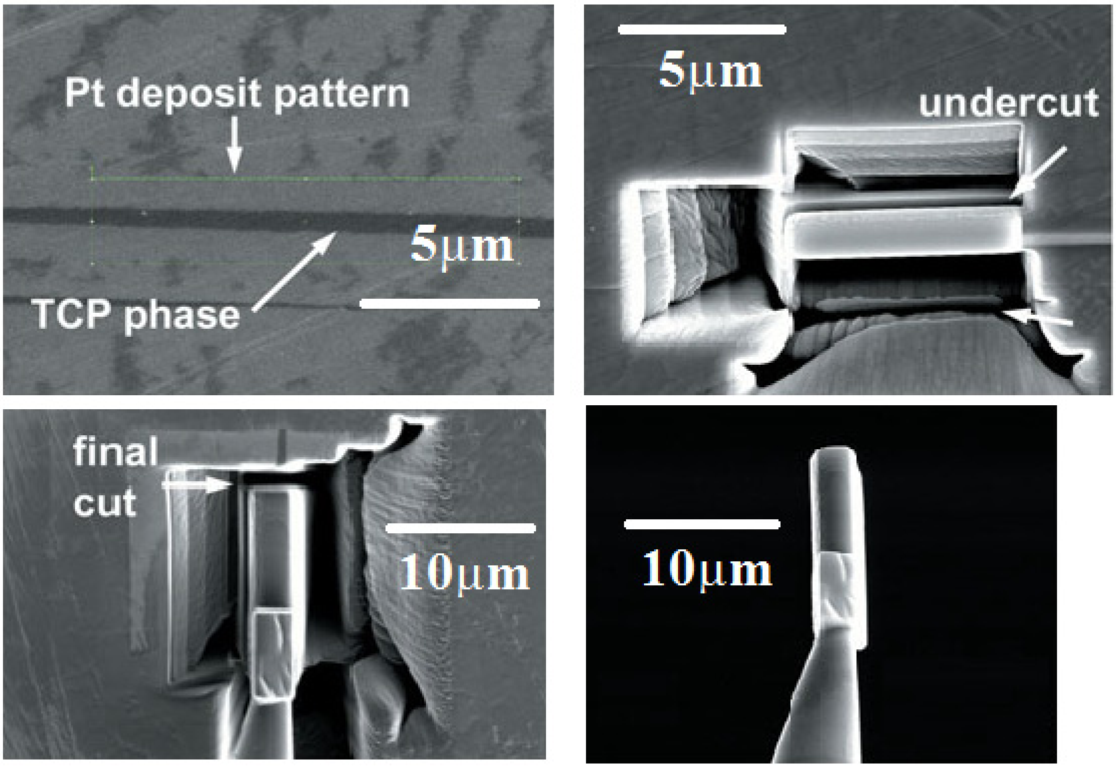

Figure 2. The FIB liftout process for APT sample preparation. Clockwise from top left: Deposition of protective Pt layer, undercut of liftout wedge, attachment of manipulator to wedge, extraction of liftout wedge. Modified from [9].

In order to form the material to be analysed from this wedge into the required geometry for APT analysis, a section of it is first mounted onto a high aspect ratio structure such as an electro-polished tungsten needle or a pre-fabricated silicon post. This wedge of material is then milled down using high energy Ga^+ ions to a needle shape tip with a diameter smaller than 100 nm as shown in Fig. 3. Low energy ions (5 kV - 2 kV) are then used to remove the damaged surface regions and ensure the region of interest is within a viable depth below the surface (50 - 100 nm) that can be reached during a typical analysis. For the analysis of specific surface regions, a capping layer of ex-situ deposited material that has been selected to match the evaporation requirements of the substrate can be used to preserve and delineate the surface [12].

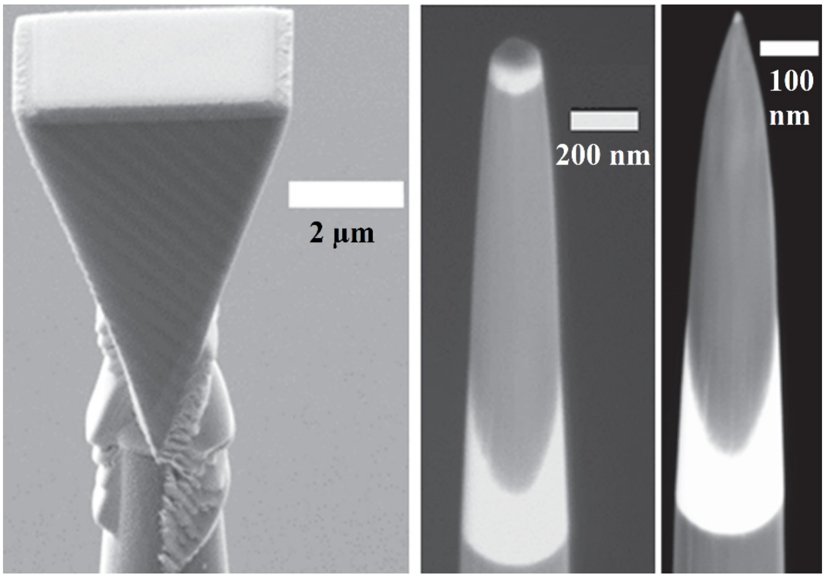

Figure 3. Section of liftout wedge mounted on silicon micropost, surface covered by protective layer of FIB deposited tungsten compound on top of capping layer of thermally evaporated cobalt (left). APT tip after 30 kV Ga^+ annular milling, cobalt layer intact (middle). Completed APT tip with ~10 nm of cobalt left to delineate surface in analysis. Modified from [12].

Selection of analysis parameters can have a large effect on the data that is collected and so a significant part of APT analysis can involve optimising these parameters, especially in a previously untested material system. There is often a balance between data quality in terms of accurate composition and spatial resolution and yield, where lower base temperatures, lower laser energies and low detection rates can lead to high data quality but at the cost of reduced yield in the form of slow data collection and increased risk of sample fracture.

Standard methodologies for reconstruction of the 3D volume from the initial raw data is carried out using a point projection method first proposed by Bas *et al.* [13]. This assumes the sample is a hemi-spherical cap on the end of a long cone and that the evaporation process is uniform across the surface, both of these assumptions can deviate significantly from reality, especially with materials with significant variation in nanoscale composition and structure [14]. Reconstructions can be informed by known crystallographic [15] or structural information (such as electron microscopy images) [16] and parameters can be altered to match these such that the reconstruction is more physical.

As the reconstruction is a point cloud, where each point has a specific location and associated mass-to-charge ratio, it is possible to use this to determine spatial relationships between different species within the reconstruction. Iso-concentration surfaces can be drawn between voxels containing specific species in order to delineate specific phases or trends in composition. 1D concentration profiles can be generated to show changes in composition over specific interfaces and proximity-histograms [17] can be used to determine changes in composition over curved surfaces such diffusion profiles between phases. When the degree of clustering or segregation is low, iso-concentration surfaces are no longer an appropriate tool and so there are a number of methods that are currently used [18] to quantity cluster composition, size and number density.

Detection limits for APT is often quoted as being in the tens of ppm, however this can vary significantly depending on the species in question, the sample, analysis conditions and the level of spatial segregation by this species. Due to the 3D nanoscale nature of APT data, a low bulk concentration species that is highly spatially segregated may have a local concentration high enough to detect if the region is extracted and analysed in isolation. APT also has the mass resolving power to measure different isotopes of elements, which is of great importance for many geological dating systems that rely on variation from natural isotopic abundancies. When trying to identify small changes in composition or the presence of low concentration species, a global mass spectrum generated from the entire dataset may not be the most appropriate as small peaks can be readily masked by larger peaks or be hidden in the variance of the global noise floor.

An advantage of the 3D visualisation of an APT mass spectrum is that localised changes in composition can be readily identified as shown in Fig. 4, where Pb species can be seen to segregate strongly in two labelled regions. The mass spectra from these volumes can then be extracted and inspected for peaks that become visible due to the reduced contribution from the global background noise and an increase in local concentration within this smaller volume. This process is shown in Fig. 5, where a much clearer mass spectra of the Pb rich region is shown on the left, with the atom map on the right showing that the core of the cluster is a combination of Y and Pb.

The accurate identification and appropriate ranging of mass spectra peaks is an important part of APT analysis in order to report reliable compositional information. This process is generally not automated and there can be significant variation between users and although there are efforts to improve consistency and reliability [20, 21].

As APT is a time-of-flight mass spectrometry technique, there can be mass spectra overlaps between species with the same mass-to-charge ratio. Deconvolution of overlapped species can be carried out by using known isotopic abundancies and can be carried on subsections on the data in order to determine the composition of specific nanoscale regions. Deconvolution can now also be carried out on an atom by atom process rather than on specific volumes [22].

There are a number of factors that limit the detection capability of specific elements. Those species that evaporate ‘off-pulse’ through field evaporation rather than ‘on-pulse’, will not be detected with a specific time-of-flight and so will appear as noise within the mass spectrum. Species such as nitrogen and oxygen are known to behave in this manner and analysis parameters such as base temperature and laser pulse energy can be optimised to reduce this issue [7].

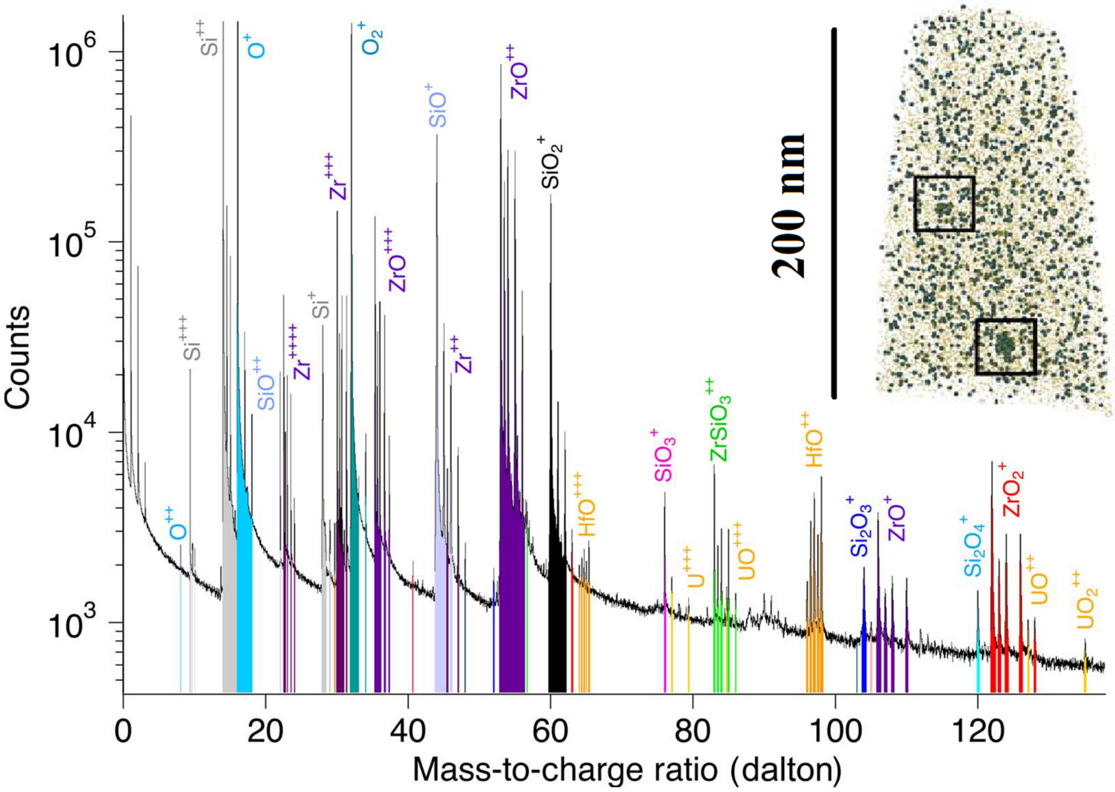

Figure 4. Global mass spectra from a discordant 2.1 Ga zircon. Species are colour coded. U (yellow), Y (orange) and Pb (green) species are shown within an atom map (inset). Localised increase in Pb highlighted in two locations. Modified from [19].

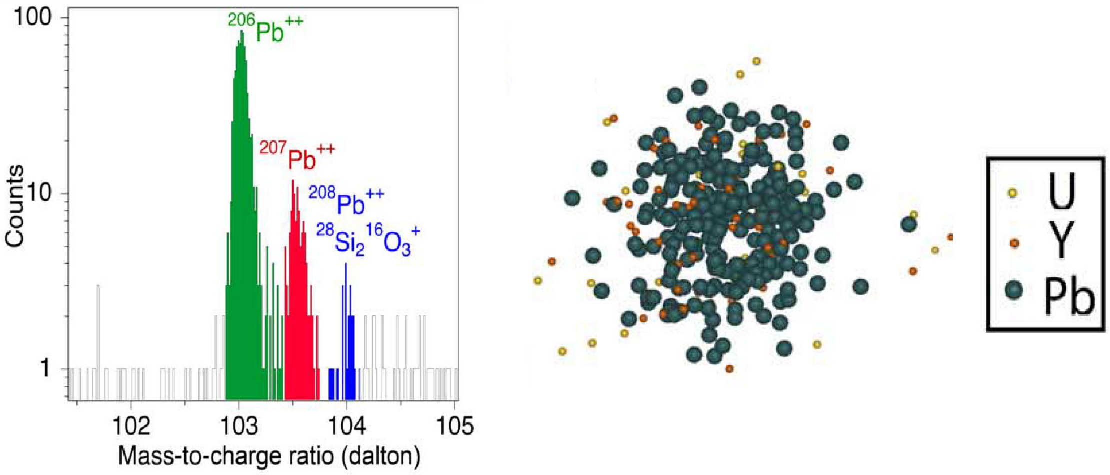

Figure 5. Local mass spectrum from Pb rich regions from Fig. 4 (left). Species are colour coded. U (yellow), Y (orange) and Pb (green) species are shown within an atom map (right). Localised increase in Pb highlighted in two locations. Modified from [19].

Hydrogen [23], oxygen, nitrogen and carbon may either be present in the analysis chamber or present on the tip prior to loading into the instrument [24] and thus may appear to be part of the sample. Variation in analysis parameters can be used in some situations to minimise the effect of these contaminants, however they may not be always removed entirely.

Generally, it can be considered that all species have equal likelihood of being detected. This is an advantage of APT over techniques such as SIMS as it means that standards are not required in order to calibrate the yield of specific species. However, the analysis parameter optimisation process can be considered to be a similar standardisation process but one that can be carried out on a sample by sample basis rather than on an independent standard. However, there can be a large variation in data collected from two otherwise compositionally identical samples due to variation in size and shape and the resultant changes to the field experienced by the tip during analysis, especially when using laser pulsing [25].

For this reason, standards of atom probe analysis parameters, reconstruction parameters (including mass spectrum ranging) and approaches to identifying and delineating features is of great importance to the atom probe community. For this reason, a number of round-robin studies have been carried out on various materials [26]. The most recent has been on a homogeneous reference zircon [27] in order to determine the differences in composition as reported by different research institutions [28]. APT samples, once they are close to their final shape and size, of a suitable size and shape that can be analysed in situ via other nanoscale analytical techniques including transmission Kikuchi diffraction (TKD) [11, 29], TEM [30] and (scanning)TEM, including associated spectroscopy techniques of EDS and elastic electron energy loss spectroscopy [31]. The additional spatial information obtained through these techniques can be used to inform the final sample preparation stages, inform the reconstruction parameters while spectroscopy techniques can be used to separate out species that cannot be resolved solely with the time-of-flight mass spectrometry data obtained through APT.

3 *ATOM PROBE OF GEOLOGICAL MATERIALS*

Initial atom probe microscopy techniques using voltage pulsing applied to geological materials in iron rich phases of the Santa Catherina meteorite were successful [32] but had limitations when applied to non-conductive regions. The advent of laser pulsing combined with advances in site specific FIB liftout techniques was a key factor in introducing APT to the analysis of geological materials. A recent review paper by Saxey *et al.* [33] is recommended for further reading on the introduction and current use of APT for geological applications.

A number of examples of the application of atom probe to geological materials are given below, the aim being to show the methodology used (especially the use of correlative microscopy) and the type of information that can be obtained using APT rather than a detailed interpretation of the data which can be found in the referenced literature.

A highly cited APT investigation of geological materials was carried out by Valley *et al.* [34] on a 4.4-Gyr-old Hadean zircon, the oldest concordant grain on Earth in order to better understand the nanoscale distribution of ^{207}Pb/^{206}Pb ratios in order to better understand its history. FIB liftouts were taken from the region of the zircon that had already been identified as having the greatest age via previous SIMS analyses.

Using iso-concentration surfaces to delineate specific volumes rich in Y from the resultant APT data (Fig. 6), Valley *et al.* [34] extracted characteristic mass spectra and compared it to the surrounding bulk. This allows a direct comparison of the composition of the matrix to clusters, showing that Pb was detectable in the form at ^{207}Pb and ^{206}Pb within the clusters. Through the unusually high ^{207}Pb/^{206}Pb ratio within the clusters compared to the bulk, they were able to determine that they formed during a later reheating event after the initial formation of the zircon. Without the combined nanoscale spatial resolution combined with high compositional sensitivity of APT, which SIMS would have blurred together with its larger analysis volume, this analysis and these conclusions could not have been reached.

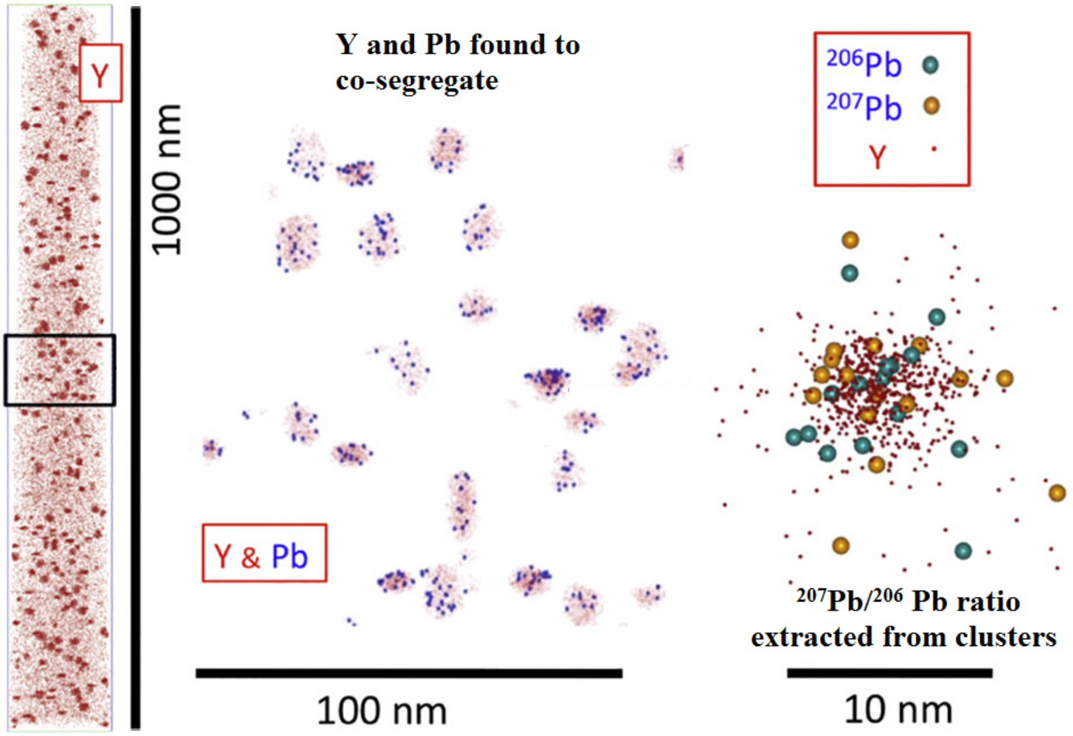

Figure 6. Y and Pb clusters within 4.4 billion year old zircon. ^{207}Pb/^{206}Pb ratios within clusters show that the Pb is radiogenic and that the clusters formed around one billion years after the zircon. Modified from [33] using data from [34] and [3].

The thermal and magnetic history of the Tazewell IAB sLH iron meteorite was investigated using a combination of APT and 3D STEM EDS [35]. It contains a complex microstructure of iron and nickel rich phases that contain information about it magnetic history over millions of years of cooling. A nanoscale intergrowth containing the naturally occurring hard ferromagnetic material, tetrataenite, has potential applications as a replacement for rare-earth magnets. This region, containing nanoscale tetrataenite islands, is known as the 'cloudy zone' and the degree of ordering of Fe-Ni within them can give information about the cooling rate. In order to determine the crystal structure and orientation of these features, STEM EDS was carried out on a needle shaped sample, similar to that required for APT. This analysis showing distinct Fe and Ni rich regions characteristic of these islands as shown in Fig. 7. APT analyses were carried out on similar samples and iso-concentration surfaces of 32.5 % Ni were used to delineate the islands as shown in Fig. 8. The plane spacing within the islands show an ordered structure but the matrix is found to be much richer in Fe than had been suggested by previous studies which proposed a pure, ordered Fe_3Ni. STEM was found to provide improved structural information over APT regarding the shape and size of the islands, as the dimensions reported by APT depend heavily on the reconstruction parameters and iso-concentration value choices. APT was found to give superior compositional information.

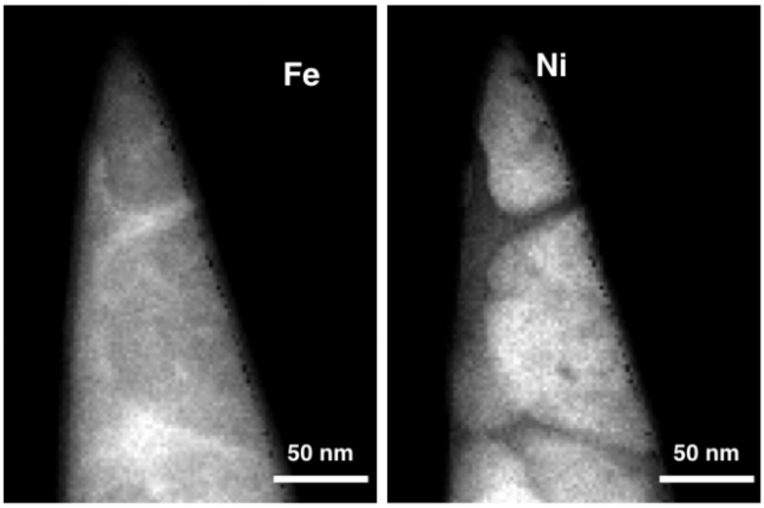

Figure 7. STEM-EDS maps of tetrataenite islands within the Tazewell IAB sLH meteorite. Modified from [35].

4. CONCLUSIONS

Modern APT, using high frequency laser pulsing and combined with advances in site specific FIB liftout, is becoming a valuable characterisation technique for geological materials. The combination of sub-nm spatial resolution with high compositional detection range within nanoscale volumes allows the analysis of segregation to crystallographic features such as grain boundaries,

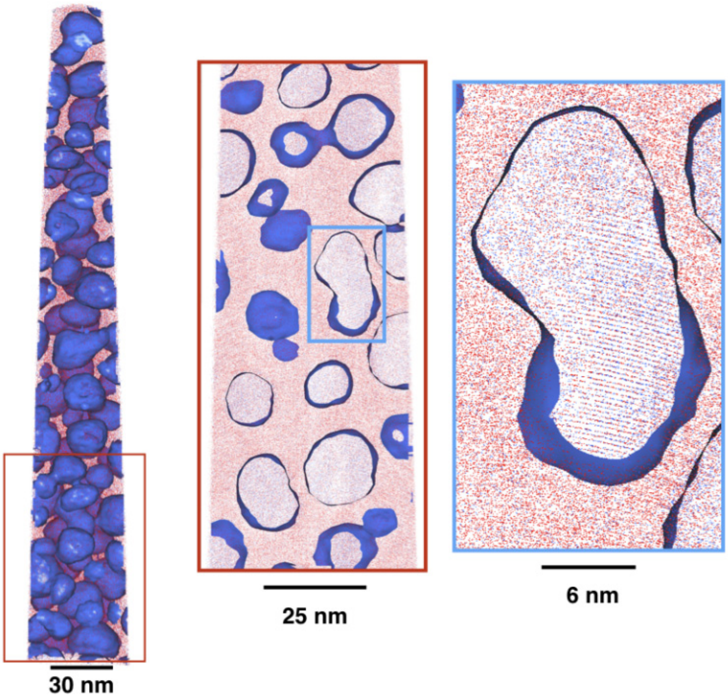

Figure 8. APT reconstruction of tetrataenite islands in increasing magnification from left to right. Modified from [35].

Dislocations, and phase interfaces. The selection of these regions of interest can be made with sub-micron precision through information gathered by complementary techniques such as EBSD and EDS during the liftout process and TKD and EDS during the final milling stages.

As APT does not require standards and will detect each element equally, it readily allows quantitative analysis of complex nanoscale features which would be difficult to obtain standards for, although care must be taken in standardising analyses between samples to ensure reproducibility. It is capable of determining variation in isotopic ratios with high precision over nanoscale distances, giving greater spatial resolution than is possible with techniques such as SIMS.

APT has successfully been applied to a variety of geological material systems, giving valuable insights into nanoscale compositional and structural information that would otherwise not be possible.

6. REFERENCES

[1] Gault B, *et al.* 2012 *Atom probe microscopy.* (New York, NY: Springer; ISBN 978-1-4614-3435-1)

[2] Larson D J, *et al.* 2013 *Local electrode atom probe tomography - A user's guide.* (New York, NY: Springer; ISBN 978-1-4614-8720-3)

[3] Valley J W, *et al.* 2015 *Amer. Mineralogist.* **100** 1355-1377
[4] Kellogg G L 1982 *J. Appl. Phys*. **53** 6383-6386
[5] Kelly T F, *et al.* 2014 *Curr. Opinion Solid State Mater. Sci.* **18** 81-89
[6] Cerezo A, *et al.* 1986 *J. Microscopy* **141** 155-170
[7] Amirifar N, *et al.* 2016 *J. Appl. Phys.* **118** 215703
[8] Larson D J and Prosa T J 2013 *Microsc. Microanal.* **19** (Suppl. 2) 994-995
[9] Miller M K, *et al.* 2007 *Microsc. Microanal.* **13** 428-436
[10] Thompson K, *et al.* 2007 *Ultramicroscopy* **107** 131-139
[11] La Fontaine A, *et al.* 2017 *Microsc. Microanal.* **23** 440-413
[12] Douglas J O, *et al.* 2016 *Semiconductor Sci. Technol.* **31** 84004
[13] Bas P, *et al.* 1995 *Appl. Surf. Sci.* **87-88** 298-304
[14] Larson D J, *et al.* 2013 *Curr. Opinion Solid State Mater. Sci.* **17** 236-247
[15] Geiser B P, *et al.* 2007 *Microsc. Microanal.* **13** 437-447
[16] Grenier A, *et al.* 2014 *Ultramicroscopy* **136** 185-192
[17] Hellman O C and Seidman D N 2002 *Mater. Sci. Engng. A* **327** 24-28
[18] Stephenson L T, *et al.* 2007 *Microsc. Microanal.* **13** 448-463
[19] Peterman E M 2016 *Science Adv.* **2** e1601318
[20] Haley D, *et al.* 2015 *Ultramicroscopy* **159** 338-345
[21] D. Hudson, *et al* 2011 *Ultramicroscopy* **111** 480-486
[22] London A J, *et al.* 2017 *Microsc. Microanal.* **23** 300-306
[23] Sundell G, *et al.* 2013 *Ultramicroscopy* **132** 285-289
[24] Zhang Y and Hillier A C 2010 *Anal. Chem.* **82** 6139-6147
[25] Bunton J H, *et al.* 2007 *Microsc. Microanal.* **13** 418-427
[26] Marquis E A, *et al.* 2016 *Microsc. Microanal.* **22** (Suppl. 3) 666-667
[27] Piazolo S, *et al.* 2017 *Chem. Geol.* **456** 101-108
[28] La Fontaine A, *et al.* 2018 *Chem. Geol.* (in press)
[29] Babinsky K, *et al.* 2015 *Ultramicroscopy* **159** 445-451
[30] Hopkin S E, *et al.* 2018 *Philosophical Mag.* **98** 766-782
[31] Meisnar M, *et al.* 2015 *Corrosion Sci.* **98** 661-671
[32] Miller M K and Russell K F 1992 *Surf. Sci.* **266** 441-445
[33] Saxey D W, *et al.* 2018 *Scripta Materialia* **148** 115-121
[34] Valley J W, *et al.* 2014 *Nature Geosci.* **7** 219-223
[35] Einsle J F, *et al.* 2018 *Proc. Natl Acad. Sci. USA* (in press)